The Linnean Society of London
ZOOLOGICAL Journal of the Linnean Society

Phylogeny and anatomy of marine mussels (Bivalvia: Mytilidae) reveal convergent evolution of siphon traits

Journal:	*Zoological Journal of the Linnean Society*
Manuscript ID	Draft
Manuscript Type:	Original Article
Keywords:	adaptation < Evolution, convergence < Evolution, Bivalvia < Taxa, Mollusca < Taxa, comparative anatomy < Anatomy, phylogenetic < Phylogenetics, character evolution < Phylogenetics
Abstract:	Convergent morphology is a strong indication of an adaptive trait. Marine mussels (Mytilidae) have long been studied for their ecology and economic importance. However, variation in lifestyle and phenotype also make them suitable models for studies focused on ecomorphological correlation and adaptation. The present study investigated the mantle margin diversity and ecological transitions in the Mytilidae to identify macroevolutionary patterns and test for convergent evolution. A fossil-calibrated phylogenetic hypothesis of Mytilidae was inferred based on five genes for 33 species (19 genera). Morphological variation in the mantle margin was examined in 43 preserved species (25 genera) and four focal species were examined for detailed anatomy. Trait evolution was investigated by ancestral state estimation and correlation tests. Our phylogeny recovered two main clades derived from an epifaunal ancestor. Subsequently, different lineages convergently shifted to other lifestyles: semi-infaunal or boring into hard substrate. Such transitions are correlated with the development of long siphons in the posterior mantle region. Two independent origins were reconstructed for the posterior lobules on the inner fold, which are associated with intense mucociliary transport, suggesting an important cleansing role in epifaunal mussels. Our results reveal new examples of convergent morphological evolution associated with lifestyle transitions in marine mussels.

ABSTRACT

Convergent morphology is a strong indication of an adaptive trait. Marine mussels (Mytilidae) have long been studied for their ecology and economic importance. However, variation in lifestyle and phenotype also make them suitable models for studies focused on ecomorphological correlation and adaptation. The present study investigated the mantle margin diversity and ecological transitions in the Mytilidae to identify macroevolutionary patterns and test for convergent evolution. A fossil-calibrated phylogenetic hypothesis of Mytilidae was inferred based on five genes for 33 species (19 genera). Morphological variation in the mantle margin was examined in 43 preserved species (25 genera) and four focal species were examined for detailed anatomy. Trait evolution was investigated by ancestral state estimation and correlation tests. Our phylogeny recovered two main clades derived from an epifaunal ancestor. Subsequently, different lineages convergently shifted to other lifestyles: semi-infaunal or boring into hard substrate. Such transitions are correlated with the development of long siphons in the posterior mantle region. Two independent origins were reconstructed for the posterior lobules on the inner fold, which are associated with intense mucociliary transport, suggesting an important cleansing role in epifaunal mussels. Our results reveal new examples of convergent morphological evolution associated with lifestyle transitions in marine mussels.

Keywords: adaptation –ancestral state – bivalves – correlation – evolutionary convergence – mantle

INTRODUCTION

Apart from their economic importance, mussels from the family Mytilidae Rafinesque, 1815 exhibit remarkable phenotypic and lifestyle diversity. These bivalves, also known as marine mussels, have an extensive fossil record, dating back to the Silurian (~427 Mya) (Berry & Boucot, 1973; Kříž, 2008). From shallow to deep waters, marine mussels represent an important benthic component in many communities, playing key ecological roles, such as colonization, bioerosion, aggregation, and supporting associated fauna (Seed *et al.*, 2000; Dinesen & Morton, 2014). Lifestyles are remarkably diverse, including epifaunal, infaunal, semi-infaunal, and boring into hard substrates (Morton, 2015). In addition, lineages of Mytilidae have proved to be suitable models for evolutionary studies, casting light on broader questions concerning adaptive radiation, diversification rates, and evolutionary novelties (Distel, 2000; Owada, 2007; Lorion *et al.*, 2013).

Many shell features and body plans within the Mytilidae are putative adaptations to either epifaunal or infaunal lifestyles (Stanley, 1972; Morton & Dinesen, 2011; Dinesen & Morton, 2014; Morton, 2015). A classic example is the calcareous borer species in the genera *Adula*, *Botula*, *Leiosolenus*, and *Lithophaga*. Despite a lack of shared history, these species have similar patterns of shell shape and chemical boring methods (Yonge, 1955; Morton & Scott, 1980; Owada, 2007, 2015; Ockelmann & Dinesen, 2009). Likewise, the adaptive radiations of deep-sea mussels on vents, seeps and organic falls are marked by convergent transitions to these deep-sea environments driven, in part, by their bacterial symbiosis (Distel et al., 2000; Jones *et al.*, 2006; Samadi *et al.*, 2007; Duperron *et al.*, 2009; Lorion *et al.*, 2010; Lorion *et al.*, 2013; Fontanez & Cavanaugh, 2013). Thus, convergence in mytilid morphology and physiology provides compelling insights into the correlation between phenotype and environment (*e.g.*, Stanley, 1972; Owada, 2007; Morton, 2015).

In this context, the mantle margin is a promising model to study convergent evolution, due to its strong association with habitat use and lineage diversification (Yonge, 1983; Audino & Marian, 2016). In bivalves, this anatomical region is usually organized in three folds responsible for sensory, muscular and secretory roles (Yonge, 1983), and often exhibits great disparity among bivalve groups. While anatomical data for the mytilid mantle margin are available for some species (*e.g.*, Soot-Ryen, 1955; Morton & Scott, 1980; Narchi & Galvão-Bueno, 1983, 1997; Morton & Dinesen, 2010; Morton, 2012; Dinesen & Morton, 2014), these data are lacking for most mytilids. Nevertheless, the observed variation in mantle margin morphology indicates that Mytilidae is a suitable model for testing hypotheses on trait evolution, correlation with lifestyles, and putative adaptations. Previous studies suggest that evolutionary convergences may have underlain morphological diversification of the family (*e.g.*, Distel, 2000). For example, siphon development would be expected among infaunal lineages as an adaptation to burrowing habits in soft sediments (Stanley, 1968).

The Mytilidae exhibit very favorable features for evolutionary investigations. The family has been consistently recovered as monophyletic and phylogenetically placed within the Pteriomorphia, along with oysters, scallops, and ark clams (Distel, 2000; Giribet & Wheeler, 2002; Matsumoto, 2003; Owada, 2007; Samadi *et al.*, 2007; Bieler *et al.*, 2014; Combosch *et al.*, 2017; Sun & Gao, 2017; Liu *et al.*, 2018; Lee *et al.*, 2019). Recent phylogenetic analyses from transcriptome and whole mitochondrial genome datasets indicate that the mytilids are organized into two major clades with high support for most genera (Gerdol *et al.*, 2017; Liu *et al.*, 2018; Lee *et al.*, 2019). However, while the relationships within some subfamilies are relatively well understood, such as the deep-sea Bathymodiolinae (Jones *et al.*, 2006; Duperron *et al.*, 2009; Lorion *et al.*, 2010; Lorion *et al.*, 2013), traditionally accepted subfamilies such as the hard-substrate borers of Lithophaginae and the Mytilinae (Distel, 2000; Owada, 2007; Gerdol *et al.*, 2017; Liu *et al.*, 2018; Lee *et al.*, 2019)

do not appear to be monophyletic. This suggests that convergent morphologies and lifestyles may be more prevalent among mytilids than expected. Such an evolutionary pattern, with pervasive morphological convergences, has been already demonstrated for other pteriomorphian clades, including Arcida and Pectinida (Oliver & Holmes 2006; Serb *et al.*, 2011; Serb *et al.*, 2017, Audino *et al.*, 2019).

To test our hypothesis that similar mytilid morphologies are likely convergent and associated with independent transitions to similar lifestyles (*i.e.*, boring, epifaunal, or infaunal),we investigated mantle evolution within Mytilidae. A phylogenetic framework was used to reconstruct the evolution of lifestyles and key mantle traits, based on extensive observations of preserved specimens, and to test hypotheses of trait correlation. In addition, we thoroughly investigated the mantle margin of two epifaunal and two borer species to explore their detailed structure and associated functions.

MATERIAL AND METHODS

Taxon sampling

A detailed history of taxonomic proposals for mytilid subfamilies was summarized by Morton (2015). The classification adopted herein is in accordance with Huber (2010, 2015), also adopted by the World Register of Marine Species (WoRMS, http://www.marinespecies.org/aphia.php?p=taxdetails&id=211), including ten subfamilies and 52 genera. We used a combination of five genes from mitochondrial (16S rRNA and COI) and nuclear (18S rRNA, 28S rRNA, and histone H3) genomes for our phylogenetic inference of the Mytilidae, totalizing 5,710 bp. Data was curated from Genbank, the public repository maintained by the National Center for Biotechnology Information (NCBI). In total, the molecular character matrix is comprised of 33 mussel species (19 genera, Table 1), including representatives of all but one subfamily (*i.e.*, Crenellinae), and has a completeness

of 79%. Eight pteriomorphian and five non-pteriomorphian bivalve species served as outgroups for the phylogenetic analyses (Table 1).

Morphology was examined in 21 of those 33 species based on preserved specimens from museum collections. For the remaining 12 sequenced species, morphological data was obtained using surrogate species within the same genus. In total we examined 43 species (25 genera) from the following collections: Museum of Comparative Zoology (MCZ), Museum of Zoology "Prof. Adão José Cardoso" of the University of Campinas (ZUEC-BIV), Museum of Zoology of the University of São Paulo (MZSP), Smithsonian National Museum of Natural History (USNM), and Santa Barbara Museum of Natural History (SBMNH). Museum catalog numbers are listed in Table 1. Specimens were dissected in ethanol and qualitative observations were made under the stereomicroscope (Table 2, supplementary Table S1).

Microscopy techniques

For detailed anatomical studies, four species were collected by hand along the São Sebastião's coast (São Paulo State, Brazil) during low tide. Specimens of *Perna perna* (Linnaeus, 1758) and *Brachidontes exustus* (Linnaeus, 1758) were collected on rocky shores and piers, while the borers *Leiosolenus aristatus* (Dillwyn, 1817) and *Leiosolenus bisulcatus* (d'Orbigny, 1853) were removed from oyster aggregations and coral fragments. All individuals were anesthetized in an isotonic 7.5% solution of $MgCl_2$ for 2 h before fixation. Fragments of the mantle margin were dissected and fixed for 3 h in a modified Karnovsky solution and stored in cacodylate buffer (Audino & Marian, 2018).

For scanning electron microscopy, samples were prepared and analyzed as described in Audino & Marian (2018). For histology, samples were completely dehydrated and embedded in glycol methacrylate resin (Leica Historesin Kit, Germany). Serial sections of 4 µm were stained by the following methods (Behmer *et al.*, 1976; Bancroft & Stevens, 1982;

Pearse, 1985): hematoxylin and eosin (HE), toluidine blue and basic fuchsin (TF), Gomori trichrome stain (GO), mercury-bromophenol blue (BB), periodic acid-Schiff (PAS), and alcian blue (AB). To recognize putative secretory cells, PAS and AB methods were used to identify mucosubstances, while BB stained protein aggregates (Bancroft & Stevens, 1982; Pearse, 1985). All histological slides were deposited at the Museum of Zoology "Prof. Adão José Cardoso" of the University of Campinas (ZUEC-BIV) under the following catalog numbers: *B. exustus* (8166–8167) *L. aristatus* (8151–8153) *L. bisulcatus* (8148–8150) *P. perna* (8164–8165).

Phylogenetic analysis and divergence time estimation

Sequence alignments were generated with MAFFT v7.311 under the L-INS-i option (Katoh & Standley, 2013). Selection of the best-fit model of nucleotide evolution was performed in ModelFinder (Kalyaanamoorthy *et al.*, 2017) under the corrected Akaike information criterion (AICc). The best fit model for the concatenate dataset was TIM + I + G. Maximum likelihood (ML) searches were conducted in IQ-TREE (Nguyen *et al.*, 2014) and node support was estimated by bootstrap with 100 replicates (Felsenstein, 1985).

Divergence times were estimated by Bayesian Inference (BI) in RevBayes under the fossilized birth-death model (Heath *et al.*, 2014; Höhna *et al.*, 2016). A relaxed molecular clock was applied assuming an uncorrelated exponential model on molecular branch rates. Posterior probabilities were sampled using the Markov Chain Monte Carlo (MCMC) method in four independent chains for 500,000 iterations. Convergence of the posteriors were verified in Tracer (Rambaut *et al.*, 2018). Fossil taxa were pruned prior to summarizing the phylogenetic trees as a maximum clade credibility tree, with a burn-in of 10%. In addition, a plot of lineages-through-time was produced in IcyTree (Vaughan, 2017).

All priors for fossil ages were drawn from uniform distributions. Occurences and ages of all fossil taxa are from the Paleobiology Database (https://paleobiodb.org/), with information verified in the corresponding publications. The root age of Bivalvia was constrained between 520.5 and 530 Mya (million years ago), based on the fossil *Fordilla troyensis* (Pojeta *et al.*, 1973). The age of Mytilidae was calibrated based on the fossils *Phthonia regularis* (427.4–425.6 Mya, Kříž, 2008) and *Mytilus* sp. (427.4–419.2 Mya) (Berry & Boucot, 1973), with ages constrained around 423.3 ± 4.1 Mya. The fossil *Bathymodiolus heretaunga*, constrained around 26.2 ± 1.1 Mya (Saether *et al.*, 2010), was used to calibrate the Bathymodiolinae. The fossil *Lithophaga subelliptica*, constrained around 301.1 ± 2.3 Mya (Newell, 1942), was used to calibrate the Lithophaginae. For the Modiolinae, the fossil *Modiolus koneckii* was constrained around 292.8 ± 2.7 Mya (Dickins 1963). The fossil *Musculus somaliensis*, constrained around 164.8 ± 1.3 Mya (Dickins 1963), was used to calibrate the Musculinae. Finally, the Mytilinae was calibrated based on the fossil *Mytilus nativus*, 244.6 ± 2.6 Mya (Konstantinov *et al.*, 2013).

Character evolution

Incurrent and excurrent apertures of mytilid mantle are traditionally treated as siphons, regardless of their level of development (Soot-Ryen, 1955). For ancestral state estimation of the excurrent siphon, we considered short siphons to be those in which the aperture is 1) wider than the length of the siphon and 2) does not form a conical structure. Alternatively, long excurrent siphons are produced by extended mantle projections, creating long conical structures. Similarly, the incurrent aperture also can form a siphon if the mantle is elongated enough to be longer than the apertures' width (i.e., conical). Mantle margin characters were coded and states were assigned to terminals based on observations of corresponding species or close relatives (Table 2; supplementary Table S1). Additional characters studied for trait

evolution include the presence of posterior projections (lobules) on the mantle margin and siphon length relative to the aperture. Ecological data (i.e., lifestyle and substrate type) were compiled from the literature (supplementary material, Table S2). Lifestyles include epifaunal (above substrate), semi-infaunal (partially buried in the sediment), infaunal (buried in the sediment) and boring (into hard substrate such as wood or limestone) (Table 2).

Ancestral state estimation (ASE) was conducted under maximum likelihood in Mesquite (Maddison & Maddison, 2018) using the ML topology. Two models for rate transition were considered: 1) the one parameter model (MK1), which assumes the same rate for all transitions, and 2) the two parameter model (AsymmMK), which allows different transition rates. A likelihood ratio test (LRT) was used to determine the model that best fits the data (Maddison & Maddison, 2018).

When two characters with multiple transitions across the phylogeny seemed to be associated with each other, a correlation test was applied to evaluate evolutionary dependence between traits (Pagel, 1994). Searches were carried out with 100 iterations and p value estimated from 10,000 simulations in Mesquite. Hypotheses of evolutionary correlation were accepted whenever the eight-parameters model presented a better fit ($p<0.05$) than the four parameters model (uncorrelated hypothesis) (Pagel, 1994; Maddison & FitzJohn, 2015).

RESULTS

Mantle margin diversity

In mytilids, the mantle margin comprises three folds. The outer and middle mantle folds are located at the distal end of the margin (Fig. 1A). These folds are usually thin and homogenous, extending along the shell margin. A thick periostracum is formed between the outer and middle folds, reaching over the outer fold to cover the external surface of the shell (Fig. 1A; thick grey line). In contrast, the inner mantle fold is proximal, being much longer

posteriorly (Fig. 1B). Despite this general pattern, the posterior mantle margin is highly variable with the type of associated structures, level of extension, and presence of pigmentation among species (Fig. 1).

Many epifaunal mussels bear posterior lobules on the inner surface of the inner fold along the incurrent aperture (arrows, Fig. 1B-E). They are usually large and folded, as observed in *Aulacomya atra* (Fig. 1B), *Mytella charruana* (Fig. 1C), all *Mytilus* species (Fig. 1D), *Mytilisepta bifurcata*, *Xenostrubus pulex*, and *Perna perna* (Fig. 2A), but may be proportionally smaller, less numerous, and sparse, like in *Septifer bilocularis, Perumytilus purpuratus*, and all *Brachidontes* species examined (Table 2, Fig. 1E).

In the posterior region, there is a point where the inner folds of the left and right mantle lobes become fused, forming an excurrent siphon. Conversely, the incurrent region does not form a delimited aperture, since the inner folds of each side do not fuse ventrally (Fig. 1B-L). Incurrent apertures forming no siphon and with wide apertures were observed in most genera, including *Mytella*, *Xenostrobus*, *Dacrydium* and those from Brachidontinae (except for *Geukensia demissa*), Bathymodiolinae, Modiolinae, and Mytilinae (Table 2). Long incurrent and excurrent siphons were observed in the boring species *Adula diengensis*, *Gregariella coralliophaga* (Fig. 1H), *Leiosolenus*, and *Lithophaga* (Fig. 1K-L), and in the semi-infaunal/infaunal mussels *Arcuatula senhousia*, *Geukensia demissa* (Fig. 1I), and *Musculus discors* (Fig. 1J) (Table 2). Generally, long siphons were greatly contracted in preserved specimens, but still very extensible when pulled up.

Beneath the incurrent aperture, close to the fusing point, there is a mantle tissue connecting the left and right mantle lobes at the base of the inner fold which also separates the excurrent and incurrent siphons. This membrane is the “basal siphonal valve” (*sensu* Carter *et al.*, 2012), and shows great morphological diversity (Fig. 1M-P) in length (relative to the length of the excurrent aperture), presence of a callus, presence of a median flap, and presence

of papillae (Table 2). The basal siphonal valve is generally shorter than the excurrent aperture in most species, forming a triangle immediately ventral to the mantle fusion point (Fig. 1M-N), as observed in *Brachidontes exustus* (Fig. 1E) and in the genera *Mytella*, *Mytilus* (Fig. 1D), and *Perna*. In other mytilids, such as *Lithophaga* and *Adula*, the basal siphonal valve is either similar in length or longer than the excurrent aperture (Fig. 1O-P). In many species, for example from the genera *Brachidontes* (Fig. 1E), *Gregariella*, and *Leiosolenus*, the central margin of the basal siphonal valve can be thick, forming a callus (Fig. 1N). In other mytilids, a median flap may be present, corresponding to a long projection that extends between the ctenidia (Fig. 1O). This is the case for *Geukensia demissa* (Fig. 1I) and *Lithophaga* species. Papillae can be distributed along the basal siphonal valve margin or on its outer surface, (Fig. 1P), as observed in *Bathymodiolus termophilus* (Fig. 1F) and most species of *Lithophaga* and *Leiosolenus*.

Functional anatomy

The mantle margin in *Perna perna* and *Brachidontes exustus* is very pigmented posteriorly and lobules are present on the inner mantle fold along the incurrent aperture (Fig. 2A-D). The siphons are very short, forming only wide apertures. The posterior lobules are intensely folded (Fig. 2A, B, D) and are covered by densely distributed, short cilia (Fig. 2C, E). The inner fold in *P. perna* contains numerous secretory cells (Fig. 2F); their content is PAS-positive, but negative to Alcian blue, indicating neutral mucosubstances. Most secretory cells occupy an inner position within the fold, with extensions to the epithelium where they release their content (Fig. 2G). The lobules also have secretory cells, although they are much less numerous (Fig. 2H). Subepithelial gland cells are abundant at the base of the inner fold and on the inner mantle epithelium of *P. perna*. These cells secrete either acid mucosubstances alone (*i.e.*, with affinity only for AB) or a mixture of acid and neutral

mucosubstances (*i.e.*, with affinity for both AB and PAS; Fig. 2I). In *Br. exustus*, secretory activity was not observed in the lobules (Fig. 2J, K). Finally, both species have very short, distally located middle folds (Fig. 2J, L). In addition, the inner epithelium of the outer fold is taller than the epithelium of the other folds, and the periostracal gland is greatly developed (Fig. 2L).

The inner folds of *Leiosolenus aristatus* and *Le. bisulcatus* are greatly enlarged, forming long siphons (Fig. 3A). The epithelium is covered by clusters of short cilia (Fig. 3B) and subepithelial secretory cells are distally located along the fold (Fig. 3C). In addition, an accessory fold is present in these species. This fold is located on the outer surface of the inner fold, forming a lateral ridge on the excurrent siphon (Fig. 3D). The surface of the accessory fold is densely covered by cilia (Fig. 3E), but no evidence of secretory activity or musculature was found (Fig. 3F). The middle and outer folds are short, originating at a distal position (Fig. 3G). Ventrally, the mantle margin contains numerous subepithelial secretory cells positive for PAS (Fig. 3H). Intense secretory activity is also present along the posterior mantle margin, close to the middle and outer folds, in a region named "posterior pallial gland". The most abundant type of secretory cell of this gland forms clusters of cells containing large granules strongly positive for PAS (Fig. 3I) and for the Fast-Green stain of the GO method (Fig. 3J); they showed weak affinity for eosin (Fig. 3K) and bromophenol blue (Fig. 3L). Interspersed with these large cells, another secretory cell type occurs; they are small cells containing granular content strongly stained by eosin (Fig. 3K), bromophenol blue (Fig. 3L), and by the acid fuchsin of the GO method (Fig. 3J). These cells are PAS-negative (Fig. 3I).

Phylogenetic hypothesis and divergence time

Mytilidae is monophyletic in our ML analysis and splits into two main clades: the first clade includes the Brachidontinae, Musculinae, Mytilinae, and Septiferinae, while the second

clade comprises the Bathymodiolinae, Dacrydinae, Modiolinae, and Lithophaginae (Fig. 4). The *Brachidontes* species are closely related to *Geukensia demissa* and *Ischadium recurvum*, and together form a clade sister to *Perumytilus* and *Mytilisepta*. The boring *Gregariella coarctata* is recovered sister to *Mytilus*, while the semi-infaunal *Musculus* and *Arcuatula senhousia* form a clade sister to the epifaunal *Perna*. Under the current taxonomic classification of mytilids, only Septiferinae was recovered as monophyletic in this main clade (Fig. 4). In the other main clade, Modiolinae is monophyletic, as well as Bathymodiolinae, which groups the deep-sea genera (Fig. 4). Interestingly, the boring species *Leiosolenus lischkei* is not sister to *Lithophaga* despite their similar habit and cylindrical shape. *Dacrydium sp*. is closely related to *Lithophaga* (although bootstraps values are low), while *Leiosolenus lischkei* is sister to the modioliform clades (Fig. 4). Considering the distant phylogenetic position between *Arcuatula senhousia* and *Xenostrobus securis*, the subfamily Arcuatulinae is not monophyletic in this analysis (Fig. 4).

The divergence time tree inferred by BI (Fig. 5) recovered the same topology as ML. The family dates back to the Silurian, around 424.3 Ma, and the two main clades diverge in the Early and Late Devonian, around 395.7 Ma and 379.9 Ma, respectively (Fig. 5). The most recent common ancestor (MRCA) dates to the Late Triassic, including, for example, the genus *Lithophaga* (205 Ma), Modiolinae (225.1 Ma), Bathymodiolinae (211.5 Ma), Brachidontinae (222.7 Ma), and Musculinae (212.7 Ma). More recent divergences during the Mesozoic include the MRCA of *Mytilus* group (182.8 Ma, Early Jurassic), *Bathymodiolus* group (128.2 Ma, Early Cretaceous), and *Perna* group (125.2 Ma, Early Cretaceous).

Character evolution

Ancestral state estimations (ASE) indicate an epifaunal ancestor for all marine mussels (Fig. 6A). Transitions to the semi-infaunal habit occurred twice, within *Modiolus* and

Geukensia. Similarly, transitions to complete infaunal habit were convergently achieved by *Dacrydium* and the ancestor of *Arcuatula* and *Musculus*. The habit of boring into hard substrate is convergent for *Gregariella*, *Leiosolenus*, and *Lithophaga*. In addition, siphon hypertrophy was investigated in combination with habits of life (Fig. 6B). According to ASE, short siphons (Fig. 6C) are plesiomorphic, and long siphons (Fig. 6D) have convergently evolved at least five times where lifestyle transition has occurred from epifaunal to either semi-infaunal, infaunal or boring (Fig. 6A, B). A correlation hypothesis was tested and returned a *p*-value of 0.03 ($p<0.05$), supporting evolutionary correlation between siphon enlargement and lifestyle transition.

The posterior lobules on the inner mantle fold have a single origin for the diverse clade including *Brachidontes*, *Mytilus*, *Mytilisepta*, *Perna*, and *Perymytilus* (Fig. 7). In addition, similar structures were also gained in *Xenostrobus* (Fig. 7). Interestingly, posterior lobules were likely lost multiple times, including in some lineages in which lifestyle shifted from epifaunal to semi-infaunal/infaunal, such as *Arcuatula+Musculus*, *Geukensia*, and *Gregariella*.

DISCUSSION

Evolutionary convergences

Similar phenotypes can evolve independently, i.e., by convergence, when unrelated lineages experience transitions to similar environments (Losos, 2011; Serb *et al.*, 2011). If repeated trait-environment associations are observed, this may indicate convergent adaptation (Losos 2011). Then, subsequent functional analyses may help identify the selective mechanism (Agrawal 2017). Phylogenetic hypotheses are essential to polarize character evolution and to identify these patterns. Besides the present contribution to mussel phylogenetics (along with other recent efforts, see Gerdol *et al.*, 2017; Liu *et al.*, 2018; Lee *et*

al., 2019), our results reveal new examples of convergent morphological evolution associated with lifestyle transitions in marine mussels.

The traditional view of mytilid evolution considers the semi-infaunal habit as the plesiomorphic condition based on endobyssate fossils with modioliform shapes (Stanley, 1972). In contrast, our ASE results suggest that mytilids evolved from an epifaunal ancestor in the Silurian. Subsequently, multiple lineages of mytilids shifted to other lifestyles in association with changes in mantle morphology. For instance, transitions to semi-infaunal, infaunal and boring habits are associated with posterior inner fold hypertrophy (*i.e.*, siphon elongation) and suggest acquisition of common adaptive phenotypes under similar ecological conditions. In addition, our results also support shifts to infaunal (*Musculus*+*Arcuatula*; Figs. 5, 6) and boring habits (*Lithophaga*; Figs. 5, 6) in the Triassic, corroborating previous hypotheses of benthic diversification and infaunalization during the Mesozoic (Vermeij, 1977). The Late Triassic is regarded as an epoch of development of an evolutionary arms race among marine groups, which characterizes the Mesozoic Marine Revolution, an era of taxonomic radiations and adaptations in response to diversification of predatory pressures (Vermeij, 1977; Harper & Skelton, 1993; Tackett & Bottjer, 2012). A similar ecomorphological pattern was identified in ark clam lineages (Arcida) that evolved longer inner folds associated with epifaunal-infaunal transitions during the Mesozoic (Audino *et al.*, 2019). These results highlight the evolvability of the mantle margin in bivalve evolution and point to trends in the radiation of marine benthic lineages.

Morphological and functional diversity of the mantle margin

While mytilid mantle margins exhibit morphological and functional diversity, we identified specific trait-environment associations. Mantle fusion in Mytilidae occurs at a single, posterior point, which corresponds to the type A described by Yonge (Yonge, 1982).

As a consequence, the mantle aperture becomes divided between a delimited excurrent siphon and a ventrally opened incurrent siphon (Fig. 6C, D). Short siphons, usually forming a wide aperture, are present among most epibyssate mussels (Table 2). They also have been reported for other epifaunal mytilid genera, such as *Benthomodiolus*, *Choromytilus*, *Limnoperna*, and *Semimytilus* (Soot-Ryen, 1955; Narchi & Galvão-Bueno, 1983, 1997; Cosel, 2002; Morton & Dinesen, 2010; Morton, 2012; Oliver, 2015). In contrast, long and extensible siphons were observed in borer species, such as *Gregariella*, *Leiosolenus*, and *Lithophaga*, as well as in the borers *Adula* and *Botula* (Soot-Ryen, 1955; Yonge, 1955; Morton & Scott, 1980; Valentich-Scott & Tongkerd, 2008; Ockelmann & Dinesen, 2009). Long siphons are also present in some semi-infaunal/infaunal species that display the byssal nest-building habit, like *Arcuatula*, *Geukensia*, and *Musculus* (Bertrand, 1971; Morton & Dinesen, 2011; Morton, 2015). Interestingly, siphons are short in the semi-infaunal *Dacrydium*, *Crenatula*, and *Mytella*. The hypertrophy of the inner fold to form long siphons is observed in most infaunal groups of bivalves and is considered an adaptive trait associated with burrowing in soft substrates (Stanley, 1968; Yonge, 1983; Audino *et al.*, 2019). Similarly, boring species create channels or galleries within the hard substrate to extend elongate siphons, with only the tip exposed through the borehole (Yonge, 1955).

Convergent glandular activity is abundant and highly specialized in species boring into calcareous substrates (Morton & Scott, 1980; Morton, 1990). Different types of glands have been described, including anterior and posterior-dorsal boring glands, posterior pallial glands, and siphonal glands (Yonge, 1955; Jaccarini *et al.*, 1968; Morton & Scott, 1980; Simone & Gonçalves, 2006). Our results on *Leiosolenus aristatus* and *Le. bisulcatus* revealed a well-developed posterior pallial gland, not detected in previous studies on *Lithophaga* species (Morton & Scott, 1980; Morton, 1993). Located along the margin leading to the outer and middle folds, this gland discharges secretions containing either polysaccharides or

eosinophilic, proteinaceous substances on the posterior mantle margin. These secretions could correspond to the calcium-binding mucoproteins described for boring mechanisms in related species (Jaccarini *et al.*, 1968). According to previous assumptions, when the mantle is extended, this secretion is used to prevent calcification of the siphonal aperture, enlarging the borehole, and inhibiting skeleton formation in species boring into live corals (Jaccarini *et al.*, 1968; Morton & Scott, 1980). The accessory fold observed on the outer surface of the inner fold in *Leiosolenus* and *Lithophaga* species may act as a channel, facilitating secretion distribution along the siphonal area by mucociliary transportation.

First described for *Mytilus edulis* (Kellogg, 1915), the morphology of the basal siphonal valve is quite diverse among Mytilidae. This structure, formed by fused projections from the inner folds, shows variable length and may exhibit papillae, a callus or a median flap. Nevertheless, few details are available and information about this region is often ignored in anatomical studies, maybe because it is difficult to examine in preserved animals. Short triangular basal siphonal valves were previously described for the epifaunal *Brachidontes*, *Mytella*, and *Perna* (Narchi & Galvão-Bueno, 1983, 1997; Morton, 2012). In contrast, a long basal siphonal valve is common among the Bathymodiolinae. While some species have numerous, well-developed papillae, e.g., *Bathymodiolus heckerae*, *Ba. thermophilus*, *Benthomodiolus erebus*, and *Gigantidas platifrons* (Cosel, 2002; Oliver, 2015), others lack them entirely, e.g., *Gigantidas childressi* and *Idas argenteus* (Cosel, 2002; Ockelmann & Dinesen, 2011). A large basal siphonal valve is supposed to restrict the size of the incurrent aperture, and thus control the inflow of large particles into the mantle cavity (Morton, 1974). The presence of numerous papillae in *Lithophaga* and *Bathymodiolus*, for example, also suggests sensory roles, but further investigation is necessary to determine possible functions. The present systematization of basal siphonal valve morphology for several species represents an important initial contribution to better understand this neglected structure and its diversity.

Posterior lobules are very enlarged in epifaunal mussels, e.g., *Mytella*, *Mytilus*, *Perna*, and *Xenostrobus* (Narchi & Galvão-Bueno, 1983, 1997, present study). Small and sparse lobules are present in *Brachidontes* and *Mytilisepta* (Morton, 2012, present study). The character evolution analyses suggest a single origin of lobules, except for a convergent gain in *Xenostrobus*. Secretory cells and cilia distribution in the inner mantle fold of *Perna perna* suggests intense secretion of mucous by this fold. Therefore, the lobules should provide mucociliary transport (Sleigh, 1989), cleaning the mantle, and preventing the entrance and accumulation of undesirable, large particles. Similarly, cilia type on the papillae of *Brachidontes exutus* are likely related to transport of mucus rafts, i.e., to carry the secreted layers of mucosubstances along the epithelium (Sleigh, 1989). In addition, lobules show contraction in response to disturbance (JAA, pers. obs.), suggesting simple mechanoreception as well. Interestingly, the fact that they were independently lost in secondarily semi-infaunal/infaunal lineages suggests an adaptive role of the posterior lobes in epifaunal bivalves.

CONCLUSION

In conclusion, our results reveal new examples of convergent morphological evolution associated with lifestyle transitions in Mytilidae, combined with increased knowledge on mantle structure and functional morphology. By characterizing the evolution of ecomorphological patterns in marine mussels, our results add to the increasing body of evidence of ecological factors driving convergent phenotypical evolution in marine invertebrates (Distel 2000; Lindgren *et al.*, 2012; Li *et al.*, 2016; Sherratt *et al.*, 2016; Sherratt *et al.*, 2017; Serb *et al.*, 2017).

ACKNOWLEDGEMENTS

The authors acknowledge funding provided by FAPESP (São Paulo Research Foundation; 2015/09519-4, 2017/01365-3). This study was financed in part by the Coordenação de Aperfeiçoamento de Pessoal de Nível Superior – Brasil (CAPES), finance code 001. This study is part of the first author's Doctorate's thesis through the Graduate Program in Zoology of the Institute of Biosciences (University of São Paulo). The authors thank the following institutions that provided materials for the development of this study: Center for Marine Biology (CEBIMar), Museum of Comparative Zoology (MCZ), Museum of Zoology "Prof. Adão José Cardoso" of the University of Campinas (ZUEC), Museum of Zoology of the University of São Paulo (MZSP), Santa Barbara Museum of Natural History (SBMNH), and Smithsonian National Museum of Natural History (USNM). This is a contribution of NP-BioMar (Research Center for Marine Biodiversity – USP).

REFERENCES

Agrawal AA. 2017. Toward a predictive framework for convergent evolution: Integrating natural history, genetic mechanisms, and consequences for the diversity of life. *The American Naturalist* 190: S1–S12. https://doi.org/10.1086/692111

Audino JA, Marian JEAR. 2016. On the evolutionary significance of the mantle margin in pteriomorphian bivalves. *American Malacological Bulletin* 34: 148–159.

https://doi.org/10.4003/006.034.0212

Audino JA, Marian JEAR. 2018. Comparative and functional anatomy of the mantle margin in ark clams and their relatives (Bivalvia: Arcoidea) supports association between morphology and life habits. *Journal of Zoology* 305: 149–162.

https://doi.org/10.1111/jzo.12544

Audino JA, Serb JM, Marian JEAR. 2019. Ark clams and relatives (Bivalvia: Arcida) show convergent morphological evolution associated with lifestyle transitions in the marine benthos. *Biological Journal of the Linnean Society* 126: 866–884.

https://doi.org/10.1093/biolinnean/blz017

Bancroft J, Stevens A. 1982. *Theory and Practice of Histological Techniques*. New York: Churchill Livingstone.

Behmer OA, Tolosa EMC, Freitas Neto AG. 1976. *Manual de técnicas para microscopia normal e patológica*. São Paulo: Edusp.

Berry WBN, Boucot AJ. 1973. Correlation of the African Silurian rocks. *Geological Society of America Special Papers* 147: 1–74.

Bertrand G. 1971. The ecology of the nest-building bivalve *Musculus lateralis* commensal with the ascidian *Molgula occidentalis*. *Veliger* 14: 23–29.

Bieler R, Mikkelsen PM, Collins TM, Glover EA, González VL, Graf DL, … Giribet G. 2014. Investigating the Bivalve Tree of Life – an exemplar-based approach combining molecular and novel morphological characters. *Invertebrate Systematics* 28: 32.

https://doi.org/10.1071/IS13010

Boss KJ. 1971. Critical estimate of the number of recent Mollusca. *Occasional Papers on Mollusks. Museum of Comparative Zoology. Harvard University* 3: 81–135.

Carter JG, Harries PJ, Malchus N, Sartori AF, Anderson LC, Bieler R, … Zieritz A. 2012. Illustrated glossary of the Bivalvia. *Treatise Online* no. 48, part N, vol. 1, 1–209.

https://doi.org/10.17161/to.v0i0.4322

Combosch DJ, Collins TM, Glover EA, Graf DL, Harper EM, Healy JM, … Bieler R. 2017. A family-level Tree of Life for bivalves based on a Sanger-sequencing approach. *Molecular Phylogenetics and Evolution* 107: 191–208. https://doi.org/10.1016/j.ympev.2016.11.003

Cosel R von. 2002. A new species of bathymodioline mussel (Mollusca, Bivalvia, Mytilidae) from Mauritania (West Africa), with comments on the genus *Bathymodiolus* Kenk & Wilson, 1985. *Zoosystema* 24: 259–271.

Dickins JM. 1963. Permian pelecypods and gastropods from western Australia. *Bulletin of the Bureau of Mineral Resources, Geology and Geophysics* 63.

Dinesen GE, Morton B. 2014. Review of the functional morphology, biology and perturbation impacts on the boreal, habitat-forming horse mussel *Modiolus modiolus* (Bivalvia: Mytilidae: Modiolinae). *Marine Biology Research* 10: 845–870. https://doi.org/10.1080/17451000.2013.866250

Distel DL. 2000. Phylogenetic relationships among Mytilidae (Bivalvia): 18S rRNA data suggest convergence in mytilid body plans. *Molecular Phylogenetics and Evolution* 15: 25–33. https://doi.org/10.1006/mpev.1999.0733

Distel DL, Baco AR, Chuang E, Morrill W, Cavanaugh C, Smith CR. 2000. Do mussels take wooden steps to deep-sea vents? *Nature* 403: 725–726. https://doi.org/10.1038/35001667

Duperron S, Lorion J, Samadi S, Gros O, Gaill F. 2009. Symbioses between deep-sea mussels (Mytilidae: Bathymodiolinae) and chemosynthetic bacteria: diversity, function and evolution. *Comptes Rendus Biologies* 332: 298–310. https://doi.org/10.1016/j.crvi.2008.08.003

Felsenstein J. 1985. Confidence limits on phylogenies: an approach using the bootstrap. *Evolution* 39: 783–791. https://doi.org/10.1111/j.1558-5646.1985.tb00420.x

Fontanez K, Cavanaugh C. 2013. Phylogenetic relationships of hydrothermal vent mussels (Bathymodiolinae) and their symbionts. *Marine Ecology Progress Series* 474: 147–154. https://doi.org/10.3354/meps10086

Gerdol M, Fujii Y, Hasan I, Koike T, Shimojo S, Spazzali F, ... Fujita H. 2017. The purplish bifurcate mussel *Mytilisepta virgata* gene expression atlas reveals a remarkable tissue functional specialization. *BMC Genomics* 18: 590.

https://doi.org/10.1186/s12864-017-4012-z

Giribet G, Wheeler W. 2002. On bivalve phylogeny: a high-level analysis of the Bivalvia (Mollusca) based on combined morphology and DNA sequence data. *Invertebrate Biology* 121: 271–324.

https://doi.org/10.1111/j.1744-7410.2002.tb00132.x

Gustafson RG. 1998. A new genus and five new species of mussels (Bivalvia, Mytilidae) from deep-sea sulfide/hydrocarbon seeps in the Gulf of Mexico. *Malacologia* 40: 63–112.

Harper EM, Skelton PW. 1993. Mesozoic revolution and bivalves. S*cripta Geologica, Special Issue* 2: 127–153.

Heath TA, Huelsenbeck JP, Stadler T. 2014. The fossilized birth–death process for coherent calibration of divergence-time estimates. *Proceedings of the National Academy of Sciences* 111: E2957–E2966. https://doi.org/10.1073/pnas.1319091111

Höhna S, Landis MJ, Heath TA, Boussau B, Lartillot N, Moore BR, ... Ronquist F. 2016. RevBayes: Bayesian phylogenetic inference using graphical models and an interactive model-specification language. *Systematic Biology* 65(4): 726–736.

https://doi.org/10.1093/sysbio/syw021

Huber M. 2010. *Compendium of Bivalves. A Full-color Guide to 3,300 of the World's Marine Bivalves. A Status on Bivalvia after 250 Years of Research*. Hackenheim: ConchBooks.

Huber M. 2015. *Compendium of Bivalves 2. A Full-color Guide to the Remaining Seven Families. A Systematic Listing of 8,500 Bivalve Species and 10,500 Synonym*. Harxheim: ConchBooks.

Jaccarini V, Bannister W, Micallef H. 1968. The pallial glands and rock boring in *Lithophaga lithophaga* (Lamellibranchia, Mytilidae). *Journal of Zoology* 154: 397–401. https://doi.org/10.1111/j.1469-7998.1968.tb01672.x

Jones WJ, Won YJ, Maas PAY, Smith PJ, Lutz RA, Vrijenhoek RC. 2006. Evolution of habitat use by deep-sea mussels. *Marine Biology* 148: 841–851. https://doi.org/10.1007/s00227-005-0115-1

Kalyaanamoorthy S, Minh BQ, Wong TK, von Haeseler A, Jermiin LS. 2017. ModelFinder: fast model selection for accurate phylogenetic estimates. *Nature Methods* 14: 587. https://doi:10.1038/nmeth.4285

Katoh K, Standley DM. 2013. MAFFT multiple sequence alignment software version 7: improvements in performance and usability. *Molecular Biology and Evolution* 30: 772–780. https://doi.org/10.1093/molbev/mst010

Kellogg JL. 1915. Ciliary mechanisms of lamellibranchs with descriptions of anatomy. *Journal of Morphology* 26: 625–701. https://doi.org/10.1002/jmor.1050260403

Kleemann K. 1990. Evolution of the chemically-boring Mytilidae (Bivalvia). In: Morton B ed. *The Bivalvia — Proceedings of a Memorial Symposium in Honour of Sir Charles Maurice Yonge, Edinburgh, 1986*. Los Angeles: Hong Kong University Press, 111–124.

Kříž J. 2008. A new bivalve community from the Lower Ludlow of the Prague Basin (Perunica, Bohemia). *Bulletin of Geosciences* 83: 237–280.

Konstantinov AG, Sobolev ES, Yadrenkin AV. 2013. Triassic stratigraphy of the eastern Laptev Sea coast and New Siberian Islands. Russian Geology and Geophysics 54(8): 792-807. https://doi.org/10.1016/j.rgg.2013.07.004

Lee Y, Kwak H, Shin J, Kim SC, Kim T, Park JK. 2019. A mitochondrial genome phylogeny of Mytilidae (Bivalvia: Mytilida). *Molecular Phylogenetics and Evolution* 106533.

https://doi.org/10.1016/j.ympev.2019.106533

Li J, Ó Foighil D, Strong EE. 2016. Commensal associations and benthic habitats shape macroevolution of the bivalve clade Galeommatoidea. *Proceedings of the Royal Society B: Biological Sciences* 283: 20161006. https://doi.org/10.1098/rspb.2016.1006

Lindgren AR, Pankey MS, Hochberg FG, Oakley TH. 2012. A multi-gene phylogeny of Cephalopoda supports convergent morphological evolution in association with multiple habitat shifts in the marine environment. *BMC Evolutionary Biology* 12: 129.

https://doi.org/10.1186/1471-2148-12-129

Liu J, Liu H, Zhang H. 2018. Phylogeny and evolutionary radiation of the marine mussels (Bivalvia: Mytilidae) based on mitochondrial and nuclear genes. *Molecular Phylogenetics and Evolution* 126: 233–240.

https://doi.org/10.1016/j.ympev.2018.04.019

Lorion J, Buge B, Cruaud C, Samadi S. 2010. New insights into diversity and evolution of deep-sea Mytilidae (Mollusca: Bivalvia). *Molecular Phylogenetics and Evolution* 57: 71–83.

https://doi.org/10.1016/j.ympev.2010.05.027

Lorion J, Kiel S, Faure B, Kawato M, Ho SYW, Marshall B, … Fujiwara Y. 2013. Adaptive radiation of chemosymbiotic deep-sea mussels. *Proceedings of the Royal Society B: Biological Sciences* 280: 20131243. https://doi.org/10.1098/rspb.2013.1243

Losos JB. 2011. Convergence, adaptation, and constraint. *Evolution* 65: 1827–1840.

https://doi.org/10.1111/j.1558-5646.2011.01289.x

Maddison WP, FitzJohn RG. 2015. The unsolved challenge to phylogenetic correlation tests for categorical characters. *Systematic Biology* 64: 127–136.

https://doi.org/10.1093/sysbio/syu070

Maddison WP, Maddison DR. 2018. Mesquite: a modular system for evolutionary analysis. Version 3.51 http://www.mesquiteproject.org.

Matsumoto M. 2003. Phylogenetic analysis of the subclass Pteriomorphia (Bivalvia) from mtDNA COI sequences. *Molecular Phylogenetics and Evolution* 27: 429–440.

https://doi.org/10.1016/S1055-7903(03)00013-7

Morton B. 1974. Some aspects of the biology, population dynamics, and functional morphology of *Musculista senhausia* Benson (Bivalvia, Mytilidae). *Pacific Science* 28: 19–33.

Morton B. 1990. Corals and their bivalve borers—the evolution of a symbiosis. In: Morton B ed. *The Bivalvia—Proceedings of a Memorial Symposium in Honour of Sir Charles Maurice Yonge, Edinburgh, 1986*. Hong Kong: Hong Kong University Press, 11–46.

Morton B. 1993. How the 'forceps' of *Lithophaga aristata* (Bivalvia: Mytiloidea) are formed. *Journal of Zoology* 229: 609–621.

https://doi.org/10.1111/j.1469-7998.1993.tb02659.x

Morton B. 2012. A significant and unappreciated intertidal mytiloidean genus: the biology and functional morphology of *Brachidontes puniceus* (Bivalvia: Mytilidae) from the Cape Verde Islands. *African Journal of Marine Science* 34: 71–80.

https://doi.org/10.2989/1814232X.2012.673285

Morton B. 2015. Evolution and adaptive radiation in the Mytiloidea (Bivalvia): clues from the pericardial–posterior byssal retractor musculature complex. *Molluscan Research* 35: 227–245.

https://doi.org/10.1080/13235818.2015.1053167

Morton B, Dinesen GE. 2010. Colonization of Asian freshwaters by the Mytilidae (Bivalvia): a comparison of *Sinomytilus harmandi* from the Tonle-Sap River, Phnom Penh, Cambodia, with *Limnoperna fortunei*. *Molluscan Research* 30: 57-72.

Morton B, Dinesen GE. 2011. The biology and functional morphology of *Modiolarca subpicta* (Bivalvia: Mytilidae: Musculinae), epizoically symbiotic with *Ascidiella aspersa* (Urochordata: Ascidiacea), from the Kattegat, northern Jutland, Denmark. *Journal of the Marine Biological Association of the United Kingdom* 91: 1637–1649. https://doi.org/10.1017/S0025315410001980

Morton B, Scott PJB. 1980. Morphological and functional specializations of the shell, musculature and pallial glands in the Lithophaginae (Mollusca: Bivalvia). *Journal of Zoology* 192: 179–203. https://doi.org/10.1111/j.1469-7998.1980.tb04229.x

Narchi W, Galvão-Bueno MS. 1983. Anatomia funcional de *Mytella charruana* (D'Orbigny, 1846) (Bivalvia: Mytilidae). *Boletim de Zoologia* 6: 113–145.

Narchi W, Galvão-Bueno MS. 1997. Functional anatomy of *Perna perna* (Linné) (bivalvia, Mytilidae). *Revista Brasileira de Zoologia* 14: 135–168. http://dx.doi.org/10.1590/S0101-81751997000100014

Newell ND. 1942. Late Paleozoic pelecypods: Mytilacea. State Geological Survey of Kansas. Volume 10, Part 2. Kansas: University of Kansas Publications.

Nguyen LT, Schmidt HA, von Haeseler A, Minh BQ. 2014. IQ-TREE: a fast and effective stochastic algorithm for estimating maximum-likelihood phylogenies. *Molecular biology and evolution* 32: 268–274. https://doi.org/10.1093/molbev/msu300

Ockelmann KW, Dinesen GE. 2009. Systematic relationship of the genus *Adula* and its descent from a *Mytilus*-like ancestor (Bivalvia, Mytilidae, Mytilinae). *Steenstrupia* 30: 141–152.

Ockelmann KW, Dinesen GE. 2011. Life on wood – the carnivorous deep-sea mussel *Idas argenteus* (Bathymodiolinae, Mytilidae, Bivalvia). *Marine Biology Research* 7: 71–84. https://doi.org/10.1080/17451001003714504

Oliver PG. 2015. Description and morphology of the "Juan de Fuca vent mussel", *Benthomodiolus erebus* sp. n. (Bivalvia, Mytilidae, Bathymodiolinae): "Phylogenetically basal but morphologically advanced". *Zoosystematics and Evolution* 91: 151–165. https://doi.org/10.3897/zse.91.5417

Oliver PG, Holmes AM. 2006. The Arcoidea (Mollusca: Bivalvia): a review of the current phenetic-based systematics. *Zoological Journal of the Linnean Society* 148(3): 237-251. https://doi.org/10.1111/j.1096-3642.2006.00256.x

Owada M. 2007. Functional morphology and phylogeny of the rock-boring bivalves *Leiosolenus* and *Lithophaga* (Bivalvia: Mytilidae): a third functional clade. *Marine Biology* 150: 853–860. https://doi.org/10.1007/s00227-006-0409-y

Owada M. 2015. Functional phenotypic plasticity of the endolithic mytilid *Leiosolenus curtus* (Lischke, 1874) (Bivalvia: Mytilidae). *Molluscan Research* 35: 188–195. https://doi.org/10.1080/13235818.2015.1052129

Pagel M. 1994. Detecting correlated evolution on phylogenies: a general method for the comparative analysis of discrete characters. *Proceedings of the Royal Society B: Biological Sciences* 255: 37–45. https://doi.org/10.1098/rspb.1994.0006

Pearse AGE. 1985. Histochemistry, theoretical and applied. Vol. 2. Analytical technology, 4th ed. London: Churchill Livingstone.

Pojeta J, Runnegar B, Kriz J. 1973. *Fordilla troyensis* Barrande: the oldest known pelecypod. *Science* 180(4088): 866–868. https://doi.org/10.1126/science.180.4088.866

Rambaut A, Drummond AJ, Xie D, Baele G, Suchard MA. 2018. Posterior summarization in Bayesian phylogenetics using Tracer 1.7. *Systematic Biology* 67: 901–904.

https://doi.org/10.1093/sysbio/syy032

Saether KP, Little CT, Campbell KA, Marshall BA, Collins M, Alfaro AC. 2010. New fossil mussels (Bivalvia: Mytilidae) from Miocene hydrocarbon seep deposits, North Island, New Zealand, with general remarks on vent and seep mussels. *Zootaxa* 2577: 1–45.

Samadi S, Quéméré E, Lorion J, Tillier A, von Cosel R, Lopez P, Cruaud C, Couloux A, Boisselier-Dubayle MC. 2007. Molecular phylogeny in mytilids supports the wooden steps to deep-sea vents hypothesis. *Comptes Rendus Biologies* 330: 446–456.

https://doi.org/10.1016/j.crvi.2007.04.001

Seed R, Richardson CA, Smith K. 2000. Marine mussels, their evolutionary success, ecological significance and use as chronometers of environmental change. *Geological Society, London, Special Publications* 177: 465–478.

https://doi.org/10.1144/GSL.SP.2000.177.01.32

Serb JM, Alejandrino A, OtáRola-Castillo E, Adams DC. 2011. Morphological convergence of shell shape in distantly related scallop species (Mollusca: Pectinidae). *Zoological Journal of the Linnean Society* 163: 571–584. https://doi.org/10.1111/j.1096-3642.2011.00707.x

Serb JM, Sherratt E, Alejandrino A, Adams DC. 2017. Phylogenetic convergence and multiple shell shape optima for gliding scallops (Bivalvia: Pectinidae). *Journal of Evolutionary Biology* 30: 1736–1747. https://doi.org/10.1111/jeb.13137

Sherratt E, Alejandrino A, Kraemer AC, Serb JM, Adams DC. 2016. Trends in the sand: Directional evolution in the shell shape of recessing scallops (Bivalvia: Pectinidae). *Evolution* 70: 2061–2073. https://doi.org/10.1111/evo.12995

Sherratt E, Serb JM, Adams DC. 2017. Rates of morphological evolution, asymmetry and morphological integration of shell shape in scallops. *BMC Evolutionary Biology* 17: https://doi.org/10.1186/s12862-017-1098-5

Simone LRL, Gonçalves EP. 2006. Anatomical study on *Myoforceps aristatus*, an invasive boring bivalve in S.E. Brazilian coast (Mytilidae). *Papéis Avulsos de Zoologia* 46: 57–65. http://dx.doi.org/10.1590/S0031-10492006000600001

Sleigh MA. 1989. Adaptations of ciliary systems for the propulsion of water and mucus. *Comparative Biochemistry and Physiology Part A: Physiology* 94: 359–364. https://doi.org/10.1016/0300-9629(89)90559-8

Soot-Ryen T. 1955. A report on the family Mytilidae (Pelecypoda). *Allan Hancock Pacific Expeditions* 20: 1–175.

Stanley SM. 1968. Post-Paleozoic adaptive radiation of infaunal bivalve molluscs: A consequence of mantle fusion and siphon formation. *Journal of Paleontology* 42: 214–229.

Stanley SM. 1972. Functional morphology and evolution of byssally attached bivalve mollusks. *Journal of Paleontology* 46: 165–212.

Sun W, Gao L. 2017. Phylogeny and comparative genomic analysis of Pteriomorphia (Mollusca: Bivalvia) based on complete mitochondrial genomes. *Marine Biology Research* 13: 255–268. https://doi.org/10.1080/17451000.2016.1257810

Tackett LS, Bottjer DJ. 2012. Faunal succession of Norian (Late Triassic) level-bottom benthos in the lombardian basin: implications for the timing, rate, and nature of the early Mesozoic marine revolutionnorian paleoecology. *Palaios* 27(8): 585–593. https://doi.org/10.2110/palo.2012.p12-028r

Trovant B, Ruzzante DE, Basso NG, Orensanz JM. 2013. Distinctness, phylogenetic relations and biogeography of intertidal mussels *(Brachidontes*, Mytilidae) from the south-western Atlantic. *Journal of the Marine Biological Association of the United Kingdom* 93: 1843–1855. https://doi.org/10.1017/S0025315413000477

Valentich-Scott P, Tongkerd P. 2008. Coral-boring bivalve molluscs of southeastern Thailand, with the description of a new species. *Raffles Bulletin of Zoology* 18: 191–216.

Vaughan TG. 2017. IcyTree: rapid browser-based visualization for phylogenetic trees and networks. *Bioinformatics* 33: 2392–2394. https://doi.org/10.1093/bioinformatics/btx155

Vermeij GJ. 1977. The Mesozoic marine revolution: evidence from snails, predators and grazers. *Paleobiology* 3: 245–258. https://doi.org/10.1017/S0094837300005352

Yonge CM. 1955. Adaptation to rock boring in *Botula* and *Lithophaga* (Lamellibranchia, Mytilidae) with a discussion on the evolution of this habit. *Journal of Cell Science* 3: 383–410.

Yonge CM. 1982. Mantle margins with a revision of siphonal types in the Bivalvia. *Journal of Molluscan Studies* 48: 102–103. https://doi.org/10.1093/oxfordjournals.mollus.a065609

Yonge CM. 1983. Symmetries and the role of the mantle margins in the bivalve Mollusca. *Malacological Review* 16: 1–10.

FIGURE LEGENDS

Figure 1. Mantle margin morphology and diversity in Mytilidae. Lateral view in (C) and (E); ventro-posterior view in (B), (D), (F-L). Posterior lobules on the inner fold are indicated by arrows. Scale bars = 1mm. (A). Schematic representation of the variation of the mantle margin along the antero-posterior axis; anterior region at top and posterior region at bottom. (B). *Aulacomya atra* (MCZ288117). (C). *Mytella charruana* (ZUECBIV2177). (D). *Mytilus californianus* (USNM802552). (E). *Brachidontes exustus* (USNM760843). (F). *Bathymodiolus termophilus* (SBMNH350528). (G). *Adula diegensis* (SBMNH83588). (H). *Gregariella coralliophaga* (MZSP96956). (I). *Geukensia demissa* (SBMNH95794). (J). *Musculus discors* (USNM832507). (K). *Lithophaga lithophaga* (MCZ271738). (L). *Lithophaga nigra* (USNM833842). (M-P). Schematic representations of the basal siphonal valve morphology (posterior view). (M). Short basal siphonal valve. (N). Short basal siphonal valve with callus. (O). Long basal siphonal valve with flap. (P). Long basal siphonal valve with papillae. Abbreviations: ca, callus; es, excurrent siphon; fl, flap; ia, incurrent aperture; if, inner mantle fold; is, incurrent siphon; ma, mantle; mf, middle mantle fold; of, outer mantle fold; pa, papillae; pe, periostracum; sh, shell; sv, basal siphonal valve.

Figure 2. Mantle margin anatomy in the mussels *Perna perna*, (A-C), (F-I), and *Brachidontes exustus*, (D), (E), (J-L). Scanning electron microscopy in (B-E), and histological sections in (F-L) evidencing secretory cells (arrows and arrowheads). (A). Incurrent aperture and posterior lobules on the inner fold, as observed in a living specimen (ventro-posterior view). (B). Detail of lobules. (C). Short cilia covering the lobule's surface. (D). Detail of a lobule. (E). Cilia distributed on lobule's surface. (F). Intense secretory content within the inner fold; PAS. (G). Detail of secretory cells opening on the outer surface of the inner fold; PAS. (H).

Secretory cells in the lobules; PAS. (I). Detail of two types of subepithelial secretory cells at the base of the inner fold and on the inner mantle epithelium: cells with AB-positive content (arrowheads), and cells containing a mixture of PAS- and AB-positive contents (arrows). (J). Section through the region where the inner folds are partially fused; TF. (K). Detail of a small lobule on the inner fold; TF. (L). Outer mantle fold and middle mantle fold with the periostracal gland located between them; GO. Abbreviations: if, inner mantle fold; lo, posterior lobules; ma, mantle; mf, middle mantle fold; mu, muscle bundles; of, outer mantle fold; pg, periostracal gland; sv, basal siphonal valve.

Figure 3. Mantle margin anatomy in the borers *Leiosolenus aristatus* (A-E), (I-L) and *Leiosolenus bisulcatus* (F-H). Scanning electron microscopy in (A), (B), (D), and (E), and histological sections in (C), (F-L) evidencing secretory cells. (A). Incurrent siphon formed by long inner folds, ventral view. (B). Detail of cilia covering the surface shown in (A). (C). Epithelium of the incurrent siphon with subepithelial secretory cells (arrows); TF. (D). Short accessory fold (arrows) on the outer surface of the inner fold. (E). Detail of cilia distributed on the accessory fold. (F). Section through the accessory fold; HE. (G). Mantle margin with longer inner fold; TF. (H). Subepithelial secretory cells with mucopolysaccharide content within the mantle margin at the ventral region of the body; PAS. (I-L). Posterior mantle glands composed of large granules (arrowheads) interspersed with small secretory cells (arrows) stained by several methods. (I). PAS. (J). GO. (K). HE. (L). BB. Abbreviations: af, accessory fold; if, inner mantle fold; mf, middle mantle fold; of, outer mantle fold.

Figure 4. Phylogenetic relationships within Mytilidae. Maximum likelihood tree of Mytilidae based on five nucleotide sequences (16S rRNA, 18S rRNA, 28S rRNA, COI, and H3). Bootstrap values are indicated at the internal nodes. Mytilidae encompasses two main clades.

Subfamily names are in accordance with the classification proposed by Huber (2015), and asterisks (*) indicate subfamilies not recovered monophyletic in this analysis.

Figure 5. Time-calibrated phylogeny of Mytilidae. Divergence time analysis under Bayesian Inference based on five genes (16S rRNA, 18S rRNA, 28S rRNA, COI, and H3) and seven fossils used to calibrate internal nodes (red circles). Red numbers indicate median ages of respective nodes. Bars indicate 95% highest posterior density intervals (HPD) for nodes of interest. Posterior probabilities different than 1.0 are indicated on nodes. A lineages-through-time plot is represented on the upper left.

Figure 6. Evolution of siphons and lifestyles in Mytilidae. Ancestral state estimation of mode of life (A) and length of the excurrent siphon relative to width (B) in Mytilidae under maximum likelihood approach and equal transition rates (MK1 model). The convergent evolution of long siphons is closely associated with independent transitions to semi-infaunal, infaunal, and boring habits. (C-D). Lateral view of the posterior mantle region depicting short (C) and long (D) siphons, respectively. Black arrows indicate excurrent currents and grey arrows indicate incurrent currents of water. Abbreviations: es, excurrent siphon; ia, incurrent aperture; incurrent siphon; ma, mantle.

Figure 7. Origin of posterior lobules on the inner mantle fold. Ancestral state estimation under maximum likelihood approach with different transition rates (AsymmMK model). The results suggest gain of posterior lobules in the clade including *Brachidontes*, *Mytilisepta*, *Mytilus*, *Perna*, and *Perymytilus*, with a likely convergent gain for *Xenostrobus securis*. Multiple losses of posterior lobules are associated with lifestyle shifts from epifaunal to semi-infaunal/infaunal, such as in *Arcuatula*, *Gregariella*, *Geukensia*, and *Musculus*.

772 TABLES

773 **Table 1.** Taxa included in the analyses. Only sequenced species were included in the phylogenetic analysis while congeneric or additional
774 species were observed for morphology. Collection catalog numbers and accession numbers in *GenBank* database are listed. Abbreviations:
775 Museum of Comparative Zoology (MCZ), Museum of Zoology "Prof. Adão José Cardoso" of the University of Campinas (ZUECBIV), Museum
776 of Zoology of the University of São Paulo (MZSP), Smithsonian National Museum of Natural History (USNM), and Santa Barbara Museum of
777 Natural History (SBMNH).

Species	**Author**	**16S**	**18S**	**28S**	**COI**	**Histone H3**	**Catalog number and collection**
Adula diegensis	(Dall, 1911)						SBMNH83588
Arcuatula senhousia	(Benson, 1842)		AB201231		HQ891093		MCZ359059
Aulacomya atra	(Molina, 1782)						USNM869293, MCZ288117
Bathymodiolus brooksi	Gustafson, Turner, Lutz & Vrijenhoek, 1998						USNM1175390
Bathymodiolus thermophilus	Kenk & B. R. Wilson, 1985	KF611760	AF221638	GU966640	GQ473715	KF720623	SBMNH350528
Benthomodiolus geikotsucola	Okutani & Miyazaki, 2007	HF545049	AB679345	HF545023	AB679346	HF545149	
Benthomodiolus lignocola	Dell, 1987	KF611733	AF221648		AY275545	HF545156	
Brachidontes adamsianus	(Dunker, 1857)						USNM802545
Brachidontes darwinianus	(d'Orbigny, 1842)			KC844370	KC844414		
Brachidontes exustus	(Linnaeus, 1758)	KX71319	KT757791	KT757838	AY621838		USNM760843, SBMNH83454

Species	Author	16S	18S	28S	COI	Histone H3	Catalog number and collection
Brachidontes rodriguezii	(d'Orbigny, 1842)		DQ640530	KC844362	KC844477		MZSP115160
Crenella decussata	(Montagu, 1808)						USNM803487
Dacrydium albidum	Pelseneer, 1903						USNM886223
Dacrydium sp.	Torell, 1859	KX713210	KX713285	KX713372	KX713456	KX713529	
Dacrydium vitreum	(Møller, 1842)						USNM831489
Geukensia demissa	(Dillwyn, 1817)	U68772	L33450	AY622004	GQ282963	U68772	SBMNH95794
Gigantidas childressi	(Gustafson, Turner, Lutz & Vrijenhoek, 1998)						USNM1263668
Gigantidas mauritanicus	(Cosel, 2002)	HF545083	AY649828	FJ890504	FJ890502	HF545126	
Gregariella coarctata	(Carpenter, 1857)		AJ414641	AJ307538			
Gregariella coralliophaga	(Gmelin, 1791)						MZSP96956, ZUECBIV4844
Idas argenteus	Jeffreys, 1876						MCZ359142
Idas washingtonius	(Bernard, 1978)	HF545073	AF221645		AY275546		
Ischadium recurvum	(Rafinesque, 1820)	KT959477		AY622009	AY621933		USNM1286864, 1286716
Leiosolenus aristatus	(Dillwyn, 1817)						USNM803979
Leiosolenus bisulcatus	(d'Orbigny, 1853)						USNM803980
Leiosolenus lischkei	M. Huber, 2010	JQ267791	AB201235	AB103123	AB076944	LC004203	
Leiosolenus malaccanus	(Reeve, 1857)						SBMNH452667
Leiosolenus plumula	(Hanley, 1843)						SBMNH213239
Lioberus castanea	*(Say, 1822)*						USNM833820
Lithophaga antillarum	(d'Orbigny, 1853)	KX713229	KX713308	KX713397		KX713550	USNM847935
Lithophaga lithophaga	(Linnaeus, 1758)	JF496757	AF120530		AF120644		USNM754499, MCZ271738

Species	Author	16S	18S	28S	COI	Histone H3	Catalog number and collection
Lithophaga nigra	(d'Orbigny, 1853)		AF124209	AB103127			USNM833842, MZSP105742
Modiolus americanus	(Leach, 1815)						USNM833854, MZSP104167
Modiolus auriculatus	(Kraus, 1848)		AJ389644	AJ307537	GQ480317		USNM836901
Modiolus carpenteri	Soot-Ryen, 1963						USNM802553
Modiolus carvalhoi	Klappenbach, 1966						ZUECBIV1134
Modiolus modiolus	(Linnaeus, 1758)	KF611732	AF124210	EF526455	HM884246		SBMNH361489
Modiolus philippinarum	(Hanley, 1843)	KY705073	AB201232		KY705073	LC004218	
Modiolus rufus	(Fischer von Waldheim, 1807)	KC429248	KC429330	KC429423	KC429094	KC429165	
Musculus discors	(Linnaeus, 1767)	KR827553	AF124206		KF643642	KP113647	USNM832507, MCZ358965
Musculus niger	(J.E. Gray, 1824)		KX713316	KX713404	KF644120		USNM847946
Mytella charruana	(d'Orbigny, 1842)						ZUECBIV2177
Mytilisepta bifurcata	(Conrad, 1837)		KJ453815	KJ453831			USNM802550, SBMNH80853
Mytilisepta virgata	(Wiegmann, 1837)	AB372228	KJ453817	KJ453832	AB076941		
Mytilus californianus	Conrad, 1837	AF317544	L33449		U68777	AY267745	USNM802552
Mytilus edulis	Linnaeus, 1758	KC429249	KC429331	KC429424	KF644190	KC429166	MZSP120321
Mytilus galloprovincialis	(Lamarck, 1819)	AF317543	L33452	AB105357	AB076943	AY267748	USNM857641, MCZ251341
Mytilus trossulus	Gould, 1850	U22879	L33453		KF643612	AY267747	SBMNH235094
Perna perna	(Linnaeus, 1758)	DQ923882	DQ640520		KU743163		MZSP107780
Perna viridis	(Linnaeus, 1758)	AB265680	EF613234		DQ917584		MZSP55599

Species	Author	16S	18S	28S	COI	Histone H3	Catalog number and collection
Perumytilus purpuratus	(Lamarck, 1819)	JQ390293	KJ453820	KJ598046	KF661934		MZSP92756, USNM869289
Septifer bilocularis	(Linnaeus, 1758)						MZSP 55012, USNM747766, 746371, MCZ301874
Vilasina seminuda	(Dall, 1897)						SBMNH85093
Xenostrobus pulex	(Lamarck, 1819)						SBMNH140005
Xenostrobus securis	(Lamarck, 1819)	AB372227	EF186014		JF430154		
Outgroup							
Anadara notabilis	(Röding, 1798)		KT757768	KT757816	AF416828	KT757863	MZSP84987, 84886
Chione elevata	(Say, 1822)	KC429298	KC429387	KC429495	KC429136	KC429219	
Glycymeris glycymeris	(Linnaeus, 1758)	KC429246	KC429328	KC429421	KC429093	KC429163	USNM794960
Lima lima	(Linnaeus, 1758)	KC429257	KC429339	KC429434	KC429101	KC429174	USNM754383
Macoma balthica	(Linnaeus, 1758)	KC429303	KC429393	KC429501	KC429141	KC429224	
Malleus albus	Lamarck, 1819	KC429252	KC429334	HQ329464	KC429097	KC429169	MZSP55595
Margaritifera margaritifera	(Linnaeus, 1758)	KC429265	AF229612	KC429443	AF303316	KC429185	
Neotrigonia lamarckii	(Gray, 1838)	KC429262	KC429345	KC429443	KC429105	KC429182	
Nucula sulcata	Bronn, 1831	KC984679	AF207642	KC984815	KC984746	KC984777	
Ostrea edulis	Linnaeus, 1758	AF052068	L49052	AF137047	AF120651	AY070151	USNM836256
Pecten maximus	(Linnaeus, 1758)	KC429258	L49053	HM630545	KC429102	EU379508	
Pinctada margaritifera	(Linnaeus, 1758)	HQ329425	AB214451	AB214466	AB259166	HQ329296	USNM836493
Pinna carnea	Gmelin, 1791	KC429255	HQ329375	KJ366067	KJ366325	KC429172	MZSP29040

778

Table 2. Mantle margin morphology and habits of life in Mytilidae species investigated in the present study, grouped according to current putative subfamilies (Huber, 2010, 2015). References for ecological information and habits are listed in the supplementary material (Table S2). The length of the basal siphonal valve is relative to the length of the excurrent aperture.

MYTILIDAE	Posterior lobules	Basal siphonal valve	Siphons	Lifestyle
Arcuatulinae				
Arcuatula senhousia	absent	short with callus	long	infaunal in sand and mudflats (byssal nest)
Mytella charruana	large and folded	short	short	semi-infaunal in mudflats
Xenostrobus pulex	large and folded	short	short	epifaunal on hard substrate
Bathymodiolinae				
Bathymodiolus brooksi	absent	short	short	epifaunal on seeps
Bathymodiolus termophilus	absent	long with flap and papillae	short	epifaunal on hydrothermal vent
Gigantidas childressi	absent	short	short	epifaunal on seeps
Idas argenteus	absent	short	short	epifaunal on whale bones and sunken wood
Brachidontinae				
Brachidontes adamsianus	short and sparse	long with callus	short	epifaunal on hard substrate
Brachidontes exustus	short and sparse	short with a callus	short	epifaunal on hard substrate
Brachidontes rodriguezii	short and sparse	long with a callus	short	epifaunal on hard substrate
Geukensia demissa	absent	long with flap	long	semi-infaunal in mudflats
Perumytilus purpuratus	short and sparse	long	short	epifaunal on hard substrate
Crenellinae				
Crenella decussata	absent	short	short	infaunal in soft substrate
Vilasina seminuda	absent	unknown	short	unknown
Dacrydinae				
Dacrydium albidum	absent	short	short	infaunal in mud
Dacrydium vitreum	absent	short	short	infaunal in mud
Lithophaginae				
Adula diengensis	absent	long	long	epifaunal in crevices
Leiosolenus aristatus	absent	long with callus and papillae	long	boring into bivalve shells and corals
Leiosolenus bisulcatus	absent	long with callus and papillae	long	boring into bivalve shells and corals
Leiosolenus malaccanus	absent	short with callus	long	boring into bivalve shells and corals
Leiosolenus plumula	absent	long with flap and papillae	long	boring into bivalve shells and calcareous rocks

MYTILIDAE	Posterior lobules	Basal siphonal valve	Siphons	Lifestyle
Lithophaga antillarum	absent	long with flap and papillae	long	boring into calcareous rocks and corals
Lithophaga lithophaga	absent	long with flap and papillae	long	boring into calcareous rocks
Lithophaga nigra	absent	long with flap	long	boring into calcareous rocks and corals
Modiolinae				
Lioberus castanea	absent	short with papillae	short	epifaunal on hard substrates
Modiolus americanus	absent	short with callus	short	epifaunal or semi-infaunal in a variety of substrates
Modiolus auriculatus	absent	long with callus	short	epifaunal on hard substrates
Modiolus carpenteri	absent	short	short	epifaunal on hard substrates
Modiolus carvalhoi	absent	short	short	epifaunal on hard substrates
Modiolus modiolus	absent	unknown	short	epifaunal or semi-infaunal in a variety of substrates
Musculinae				
Gregariella coralliophaga	absent	long with callus	long	semi-infaunal or boring into hard substrates
Musculus discors	absent	short	long	infaunal in sand, mud or algae (byssal nest)
Musculus niger	absent	short	long	infaunal in sand (byssal nest)
Mytilinae				
Aulacomya atra	large and folded	short	short	epifaunal on hard substrates
Ischadium recurvum	absent	short with flap	short	epifaunal on hard substrates
Mytilus californianus	large and folded	short with callus	short	epifaunal on hard substrates
Mytilus edulis	large and folded	short	short	epifaunal on hard substrates
Mytilus galloprovincialis	large and folded	short	short	epifaunal on hard substrates
Mytilus trossulus	large and folded	short with callus	short	epifaunal on hard substrates
Perna perna	large and folded	short	short	epifaunal on hard substrates
Perna viridis	absent	short with callus	short	epifaunal on hard substrates
Septiferinae				
Mytilisepta bifurcata	large and folded	short	short	epifaunal on hard substrates
Septifer bilocularis	short and sparse	short	short	epifaunal on hard substrates

782

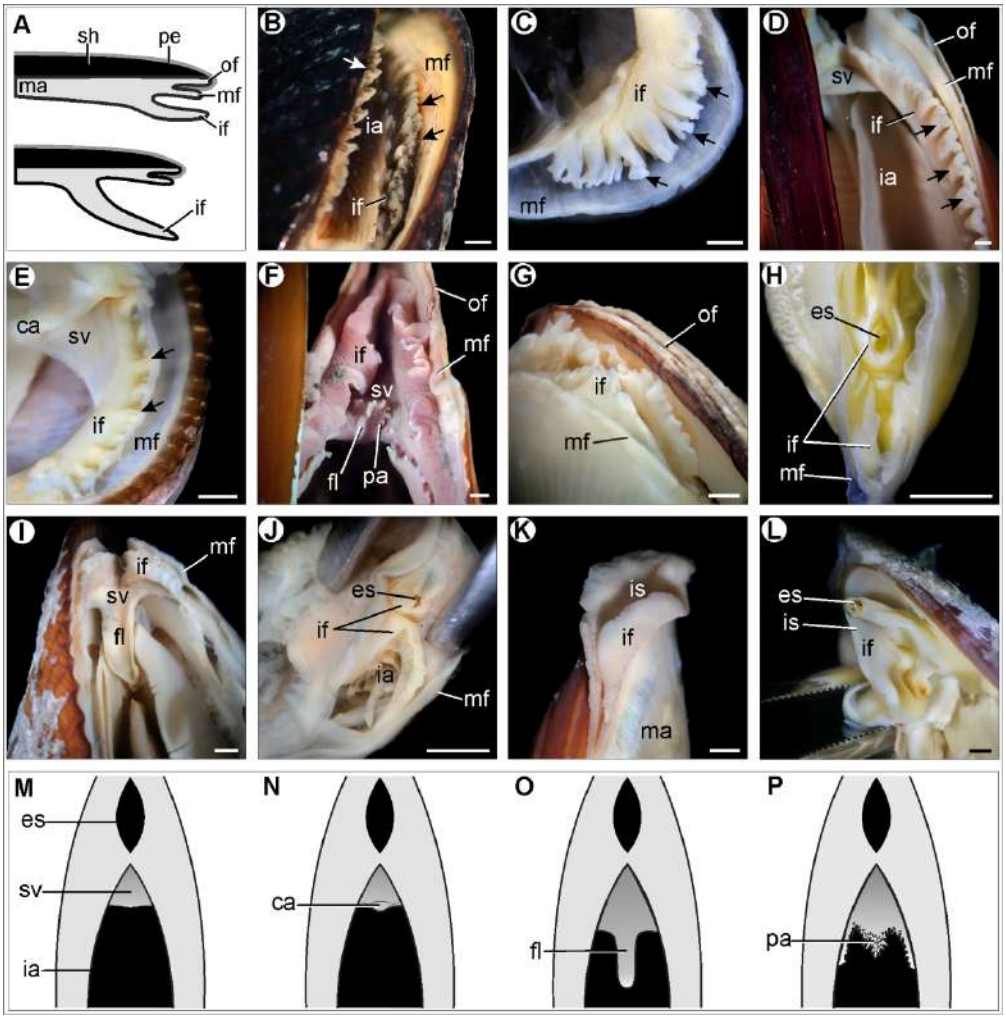

Figure 1. Mantle margin morphology and diversity in Mytilidae. Lateral view in (C) and (E); ventro-posterior view in (B), (D), (F-L). Posterior lobules on the inner fold are indicated by arrows. Scale bars = 1mm. (A). Schematic representation of the variation of the mantle margin along the antero-posterior axis; anterior region at top and posterior region at bottom. (B). *Aulacomya atra* (MCZ288117). (C). *Mytella charruana* (ZUECBIV2177). (D). *Mytilus californianus* (USNM802552). (E). *Brachidontes exustus* (USNM760843). (F). *Bathymodiolus termophilus* (SBMNH350528). (G). *Adula diegensis* (SBMNH83588). (H). *Gregariella coralliophaga* (MZSP96956). (I). *Geukensia demissa* (SBMNH95794). (J). *Musculus discors* (USNM832507). (K). *Lithophaga lithophaga* (MCZ271738). (L). *Lithophaga nigra* (USNM833842). (M-P). Schematic representations of the basal siphonal valve morphology (posterior view). (M). Short basal siphonal valve. (N). Short basal siphonal valve with callus. (O). Long basal siphonal valve with flap. (P). Long basal siphonal valve with papillae. Abbreviations: ca, callus; es, excurrent siphon; fl, flap; ia, incurrent aperture; if, inner mantle fold; is, incurrent siphon; ma, mantle; mf, middle mantle fold; of, outer mantle fold; pa, papillae; pe, periostracum; sh, shell; sv, basal siphonal valve.

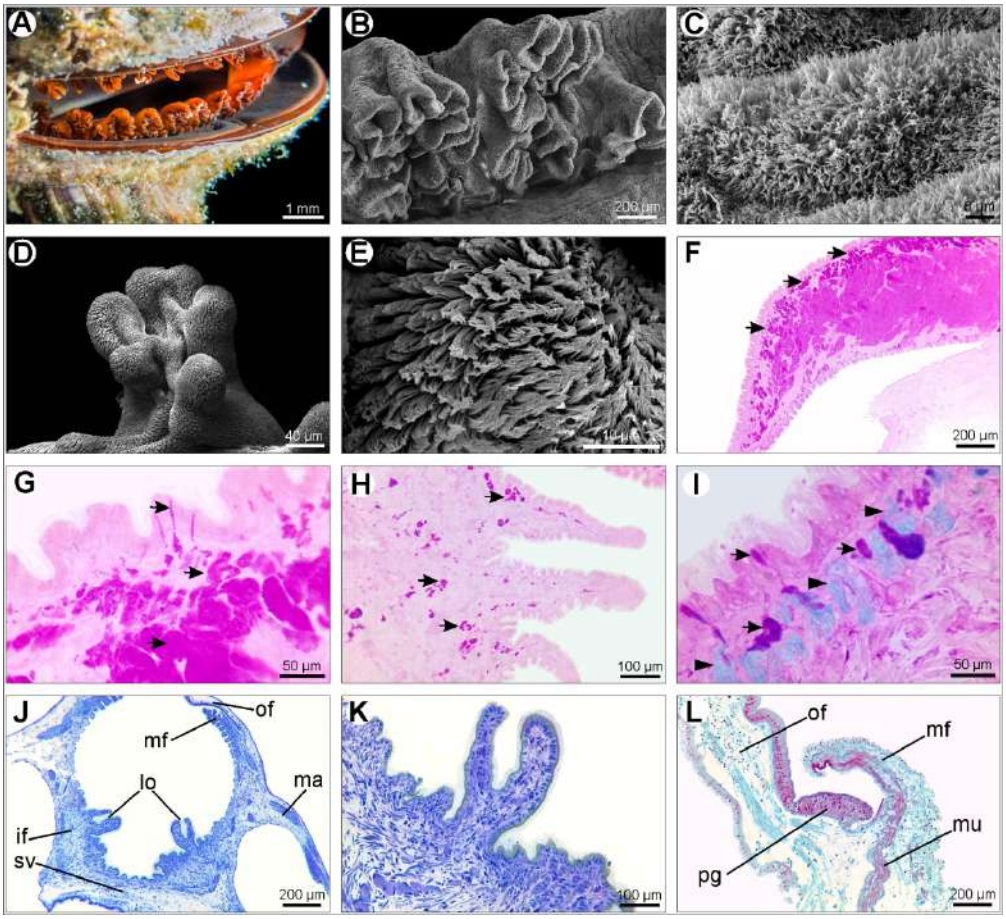

Figure 2. Mantle margin anatomy in the mussels *Perna perna*, (A-C), (F-I), and *Brachidontes exustus*, (D), (E), (J-L). Scanning electron microscopy in (B-E), and histological sections in (F-L) evidencing secretory cells (arrows and arrowheads). (A). Incurrent aperture and posterior lobules on the inner fold, as observed in a living specimen (ventro-posterior view). (B). Detail of lobules. (C). Short cilia covering the lobule's surface. (D). Detail of a lobule. (E). Cilia distributed on lobule's surface. (F). Intense secretory content within the inner fold; PAS. (G). Detail of secretory cells opening on the outer surface of the inner fold; PAS. (H). Secretory cells in the lobules; PAS. (I). Detail of two types of subepithelial secretory cells at the base of the inner fold and on the inner mantle epithelium: cells with AB-positive content (arrowheads), and cells containing a mixture of PAS- and AB-positive contents (arrows). (J). Section through the region where the inner folds are partially fused; TF. (K). Detail of a small lobule on the inner fold; TF. (L). Outer mantle fold and middle mantle fold with the periostracal gland located between them; GO. Abbreviations: if, inner mantle fold; lo, posterior lobules; ma, mantle; mf, middle mantle fold; mu, muscle bundles; of, outer mantle fold; pg, periostracal gland; sv, basal siphonal valve.

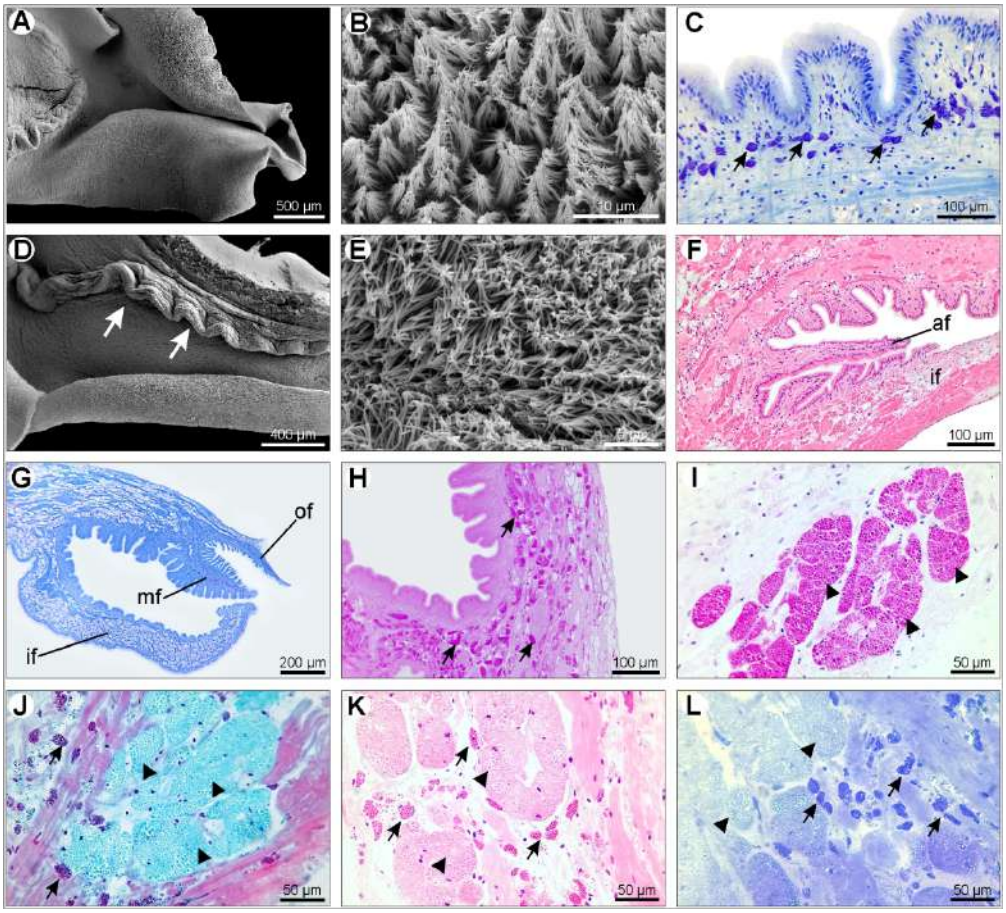

Figure 3. Mantle margin anatomy in the borers *Leiosolenus aristatus* (A-E), (I-L) and *Leiosolenus bisulcatus* (F-H). Scanning electron microscopy in (A), (B), (D), and (E), and histological sections in (C), (F-L) evidencing secretory cells. (A). Incurrent siphon formed by long inner folds, ventral view. (B). Detail of cilia covering the surface shown in (A). (C). Epithelium of the incurrent siphon with subepithelial secretory cells (arrows); TF. (D). Short accessory fold (arrows) on the outer surface of the inner fold. (E). Detail of cilia distributed on the accessory fold. (F). Section through the accessory fold; HE. (G). Mantle margin with longer inner fold; TF. (H). Subepithelial secretory cells with mucopolysaccharide content within the mantle margin at the ventral region of the body; PAS. (I-L). Posterior mantle glands composed of large granules (arrowheads) interspersed with small secretory cells (arrows) stained by several methods. (I). PAS. (J). GO. (K). HE. (L). BB. Abbreviations: af, accessory fold; if, inner mantle fold; mf, middle mantle fold; of, outer mantle fold.

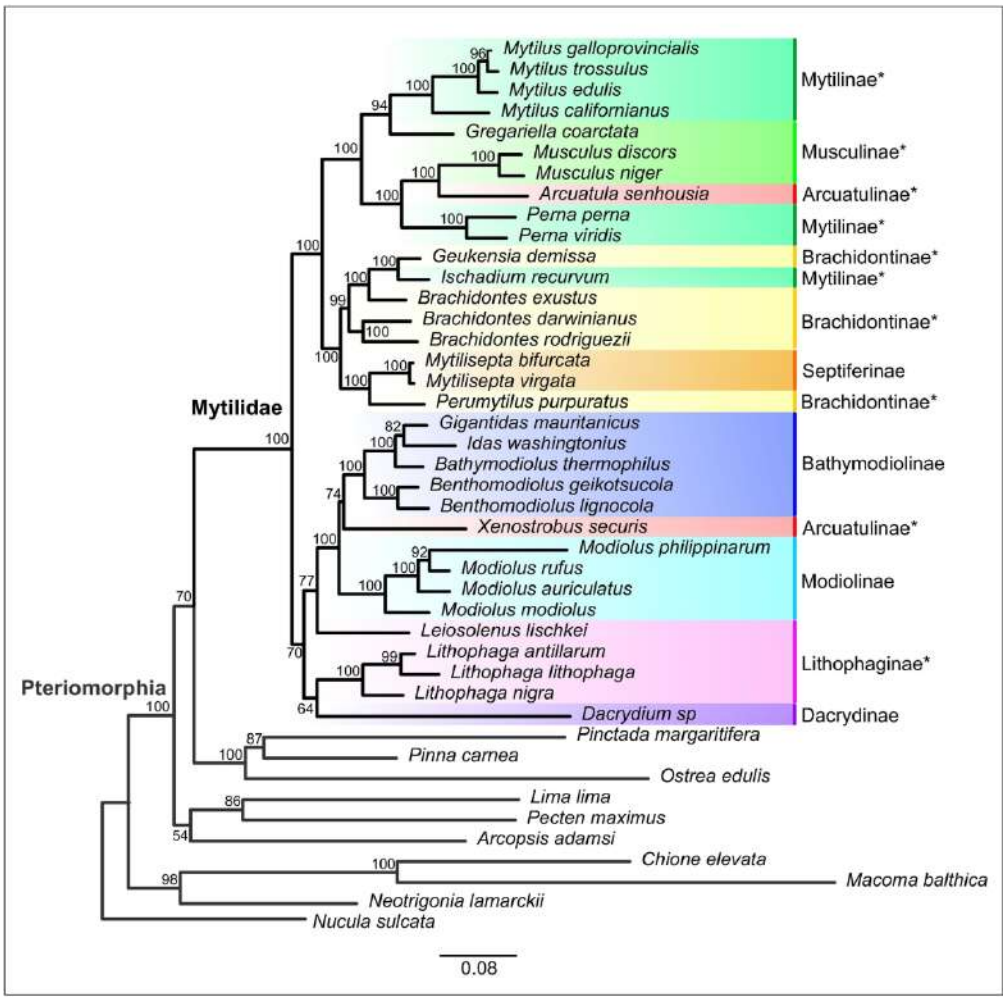

Phylogenetic relationships within Mytilidae. Maximum likelihood tree of Mytilidae based on five nucleotide sequences (16S rRNA, 18S rRNA, 28S rRNA, COI, and H3). Bootstrap values are indicated at the internal nodes. Mytilidae encompasses two main clades. Subfamily names are in accordance with the classification proposed by Huber (2015), and asterisks (*) indicate subfamilies not recovered monophyletic in this analysis.

168x166mm (300 x 300 DPI)

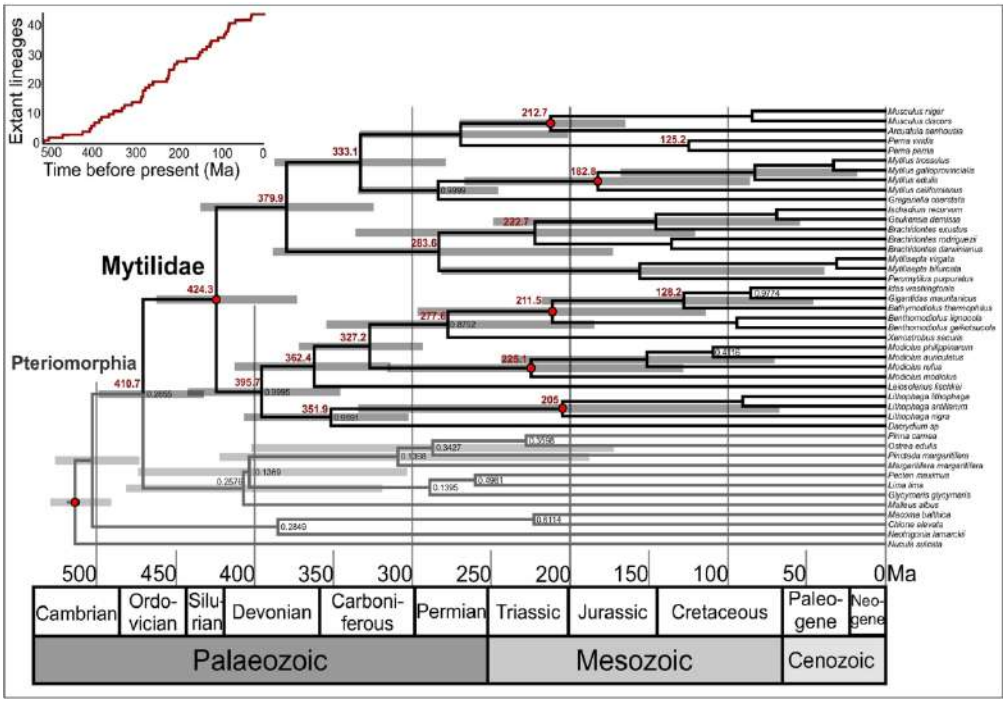

Figure 5. Time-calibrated phylogeny of Mytilidae. Divergence time analysis under Bayesian Inference based on five genes (16S rRNA, 18S rRNA, 28S rRNA, COI, and H3) and seven fossils used to calibrate internal nodes (red circles). Red numbers indicate median ages of respective nodes. Bars indicate 95% highest posterior density intervals (HPD) for nodes of interest. Posterior probabilities different than 1.0 are indicated on nodes. A lineages-through-time plot is represented on the upper left.

168x117mm (300 x 300 DPI)

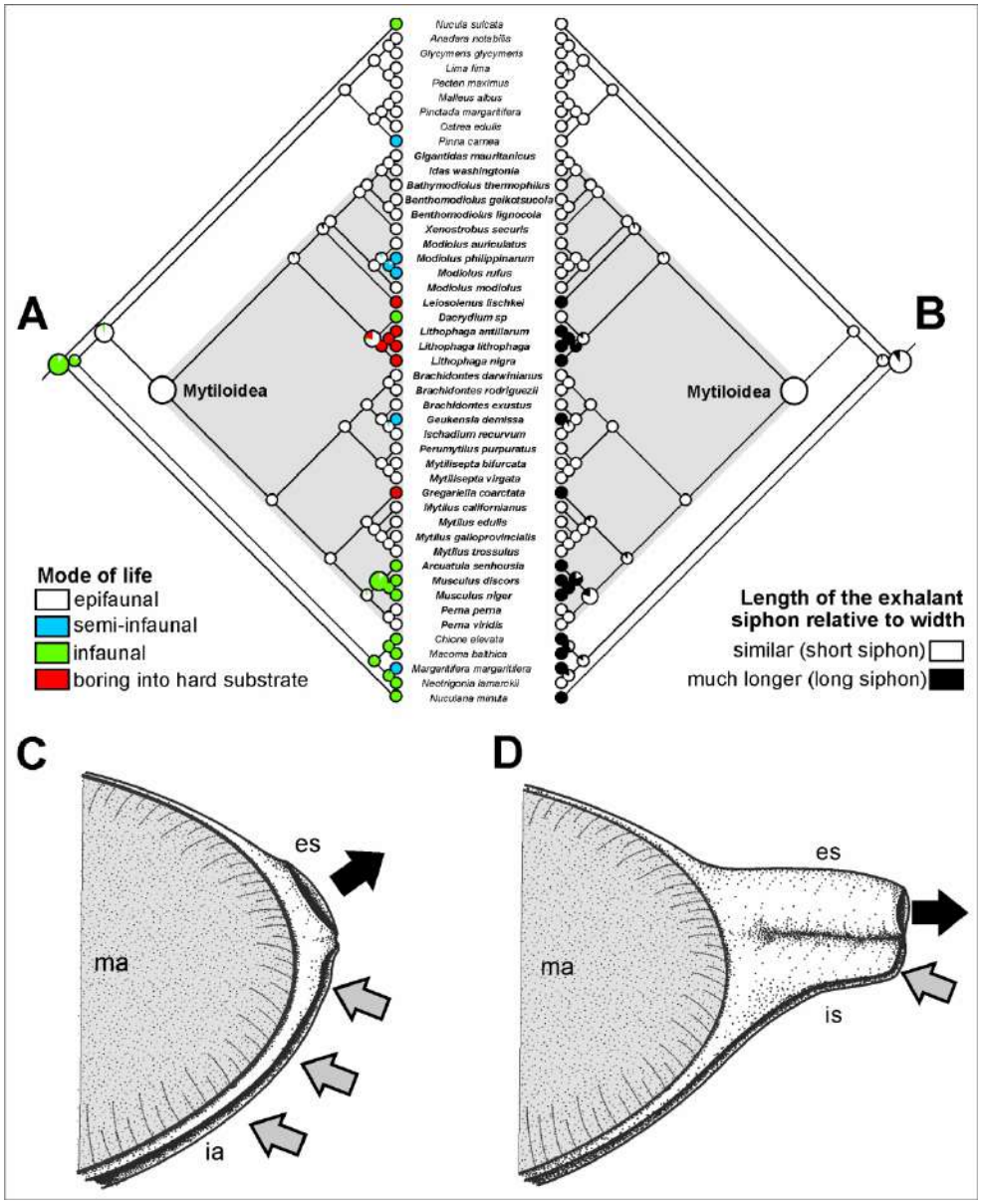

Figure 6. Evolution of siphons and lifestyles in Mytilidae. Ancestral state estimation of mode of life (A) and length of the excurrent siphon relative to width (B) in Mytilidae under maximum likelihood approach and equal transition rates (MK1 model). The convergent evolution of long siphons is closely associated with independent transitions to semi-infaunal, infaunal, and boring habits. (C-D). Lateral view of the posterior mantle region depicting short (C) and long (D) siphons, respectively. Black arrows indicate excurrent currents and grey arrows indicate incurrent currents of water. Abbreviations: es, excurrent siphon; ia, incurrent aperture; incurrent siphon; ma, mantle.

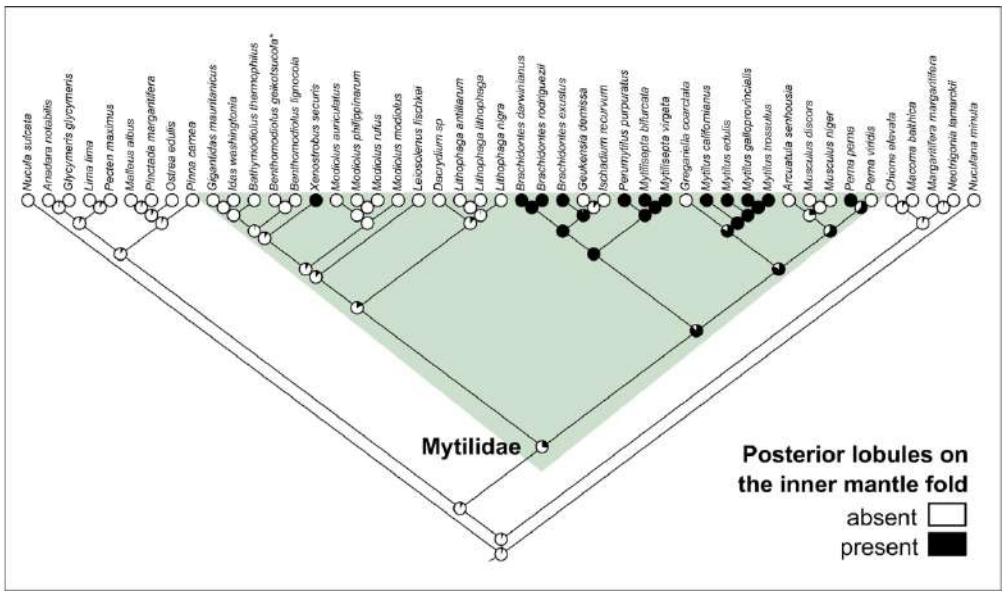

Figure 7. Origin of posterior lobules on the inner mantle fold. Ancestral state estimation under maximum likelihood approach with different transition rates (AsymmMK model). The results suggest gain of posterior lobules in the clade including *Brachidontes*, *Mytilisepta*, *Mytilus*, *Perna*, and *Perymytilus*, with a likely convergent gain for *Xenostrobus securis*. Multiple losses of posterior lobules are associated with lifestyle shifts from epifaunal to semi-infaunal/infaunal, such as in *Arcuatula*, *Gregariella*, *Geukensia*, and *Musculus*.

168x98mm (300 x 300 DPI)